Journal of Insights in Basic and Applied Sciences
مجلة رؤى في العلوم الأساسية والتطبيقية
ISSN: 3106-1737
Volume 2, Issue 3, 2026, Pages: 194-206
Journal homepage: https://jibas.com.ly/index.php/jibas/en

In Silico Evaluation and ADMET Profiling of *Silybum marianum* Bioactive Compounds as Selective COX-2 Inhibitors

Amr Ahmed [1 *], Obiyda Ahtiwesh [2], Rayan Safar [3], Shaima Alruwaye[4], Estbrak Alruwaye[5]

[1] Medical Laboratories, Faculty of Medical Technology, Nalut University, Nalut, Libya
[2,3,4,5] Department of Pharmacy, Rowad Alelm University, Tripoli, Libya

التقييم الحاسوبي وتحديد خصائص ADMET للمركبات النشطة بيولوجياً في نبات السلبين المريمي كمثبطات انتقائية لإنزيم COX-2

عمر أحمد[1*]، عبيدة احتيوش[2]، ريان صفر[3]، شيماء الرويعي[4]، إستبرق الرويعي[5]
[1] المختبرات الطبية، كلية التقنية الطبية، جامعة نالوت، نالوت، ليبيا
[2،3،4،5] قسم الصيدلة، جامعة رواد العلم، ليبيا

*Corresponding author: omar.alhrabey@gmail.com

Received: May 26, 2026	Accepted: June 27, 2026	Published: July 22, 2026

Abstract:
Long-term administration of selective COX-2 inhibitors from synthetic sources faces restrictions owing to adverse effects on cardiovascular and digestive system, maintaining the focus on designing different and natural compounds which would exhibit better isoform selectivity. Silybum marianum is abundant with various flavonolignan and flavonoid phytoconstituents which have shown some anti-inflammatory effect; however, their potential for isoform-specific selectivity of binding to COX-2 enzyme and oral bioavailability still needs to be investigated systematically. To compare S. marianum phytoconstituents regarding their selectivity towards COX-1/COX-2 isoforms, active site interactions and pharmacokinetic/toxicological characteristics compared to nine NSAID and coxib drugs. Docking of twelve phytoconstituents was performed against COX-2 enzyme and its counterpart COX-1 enzyme using PyRx 0.8/AutoDock Vina. The degree of isoform selectivity was calculated through SI (Selectivity Index) and hierarchical clustering by Z-score normalization method. Pose reproducibility was evaluated using RMSD distance between separate docking experiments aligned in PyMOL. ADMET analysis and druglikeness were predicted through SwissADME while toxicity with ProTox-II. Taxifolin ($\Delta G = -9.8$ kcal/mol; SI = 1.13) and quercetin ($\Delta G = -9.7$ kcal/mol; SI = 1.10) were the only phytoconstituents demonstrating COX-2 selective efficacy equivalent to clinically used coxibs (SI 1.13-1.27), stabilized by conserved interactions with Ser339 and Val509 resembling those in the binding pocket of celecoxib. Furthermore, taxifolin and quercetin possessed high oral bioavailability and Lipinski compliance, unlike larger flavonolignans, which suffered from a high topological polar surface area (TPSA > 150 Å²). The majority of phytoconstituents had a low toxicity profile ($LD_{50} \geq 2000$ mg/kg), with the exception of quercetin (LD_{50} = 159 mg/kg). Thus, taxifolin and quercetin can be considered structurally validated and pharmacokinetically suitable anti-inflammatory drug candidates targeting COX-2, providing an alternative approach from common silymarin formulations.

Keywords: COX-2, molecular docking, *Silybum marianum*, taxifolin, quercetin, isoform selectivity, ADMET.

الملخص:

يواجه الاستخدام طويل الأمد لمثبطات إنزيم Cyclooxygenase-2 (COX-2) الانتقائية المصنعة كيميائياً قيوداً عدة نتيجة لآثارها الضارة على القلب والأوعية الدموية والجهاز الهضمي؛ مما يُبقي التركيز مستمراً على تصميم مركبات مختلفة وطبيعية تُبدي انتقائية أفضل للأشكال المتعددة من الإنزيم. يزخر نبات حليب الشوك (Silybum marianum) بالعديد من المكونات النباتية من الفلافونوليغنان والفلافونويد التي أظهرت تأثيراً مضاداً للالتهاب؛ ومع ذلك، لا تزال قدرتها على الارتباط الانتقائي بإنزيم COX-2 وتوافرها الحيوي الفموي بحاجة إلى دراسة منهجية. تهدف هذه الدراسة إلى مقارنة المكونات النباتية لنبات حليب الشوك من حيث انتقائيتها تجاه أشكال إنزيمCOX-1/COX-2 ، وتفاعلات الموقع النشط، والخصائص الحركية الدوائية والسمية، وذلك بمقارنتها بتسعة من مضادات الالتهاب غير الستيرويدية (NSAIDs) وأدوية الكوكسيب(coxibs). أُجريت عملية الإرساء الجزيئي (Docking) لاثني عشر مكوناً نباتياً مقابل إنزيم COX-2 ونظيره إنزيم COX-1 باستخدام برنامج .PyRx 0.8/AutoDock Vina وتم حساب درجة الانتقائية للأشكال الإنزيمية من خلال مؤشر الانتقائية (SI) والتجميع الهرمي باستخدام طريقة تطبيع الدرجة المعيارية (Z-score). كما جرى تقييم تكرارية وضعية الارتباط باستخدام مسافة جذر متوسط مربعات الانحراف (RMSD) بين تجارب الإرساء المنفصلة في برنامج PyMOL. ونُفذ تحليل ADMET (الامتصاص والتوزيع والتمثيل الغذائي والإفراز والسمية) وتوقع الخصائص الشبيهة بالأدوية عبر منصة SwissADME ، بينما تم تقدير السمية بواسطة برنامج ProTox-II.أظهر التاكسيفولين قيم ($\Delta G = -9.8$ kcal/mol; SI = 1.13) والكويرسيتين قيم ($\Delta G = -9.7$ kcal/mol; SI = 1.10) أنهما المكونان الوحيدان اللذان أظهرا فعالية انتقائية تجاه COX-2 تعادل أدوية "الكوكسيب" المستخدمة سريرياً (SI 1.13-1.27) ، حيث استقرا من خلال تفاعلات مع الأحماض الأمينية Ser339 و Val509 بشكل يشبه جيب الارتباط الخاص بدواء السيلكوكسيب .(celecoxib) علاوة على ذلك، امتلك التاكسيفولين والكويرسيتين توافراً حيوياً فموياً عالياً وامتثالاً لقواعد "ليبينسكي(Lipinski) "، على عكس الفلافونوليغنانات الأكبر حجماً التي عانت من ارتفاع مساحة السطح القطبي الطوبولوجي .(TPSA > 150 Å²) أظهرت غالبية المكونات النباتية نتائج منخفضة السمية (الجرعة المميتة الوسطية LD50 ≥ 2000 ملجم/كجم)، باستثناء الكويرسيتين(LD50 = 159 mg/Kg) .وبناءً على ذلك، يمكن اعتبار التاكسيفولين والكويرسيتين مرشحين دوائيين مضادين للالتهاب يستهدفان إنزيمCOX-2 ، حيث تم إثبات فعاليتهما هيكلياً وملاءمتهما حركياً، مما يوفر نهجاً بديلاً لتركيبات السيليمارين الشائعة.

الكلمات المفتاحية: COX-2، الالتحام الجزيئي، السلبين المريمي، تاكسيفولين، كويرسيتين، ADMET

Introduction

Inflammation is an adaptive process that turns pathologic when it leads to a chronic state due to dysregulation, resulting in such pathologies as arthritis, cardiovascular disorders, and cancer [1,2,3]. Chronic inflammation is treated using mainly NSAIDs and coxibs, thus making the risk-to-benefit ratio of these drugs an important factor in the outcome of many patients; even slight advances in their selectivity and tolerance become especially significant in terms of public health despite their pharmacological unremarkableness. Among these components, the crucial player involved in the process of amplification is the cyclooxygenase-2 (COX-2), an inducible enzyme responsible for converting arachidonic acid into prostaglandin H2 (PGH2), the common precursor of inflammatory prostanoids, such as PGE2 [4]. The transcription of the COX-2 gene is predominantly controlled by NF-κB activation, thus connecting oxidative stress and cytokine signaling (IL-1β, TNF-α) with continuous prostaglandin production [5,6,7]. In addition to COX-2 induction, the process of further amplification of the inflammatory cascade is performed via complement activation, toll-like receptor signaling and secretion of TNF-α and IL-1β, ensuring continuous PGE2 production and the connection between the innate immune response and the inflammation process [8,9]. Furthermore, the COX-2 enzyme also plays the role of the cell survival and proliferation stimulator regardless of the prostaglandin synthesis process [4].

COX-2 selective inhibitors were designed to block this induced enzyme activity without affecting the continuously expressed COX-1 isoform that helps maintain the integrity of the gastric mucosa and the platelet TXA2 synthesis [10,11]. The practical result of such selectivity, however, is the disruption of the physiological equilibrium between prostacyclin (PGI2) and TXA2: the former is inhibited in the endothelial tissue while the latter continues being produced by COX-1 in the platelets, leading to a prothrombotic effect responsible for the withdrawal from the market of rofecoxib and valdecoxib as well as current safety concerns about etoricoxib among other coxibs, including Stevens-Johnson syndrome [12,13]. Such safety issues that represent an intrinsic design problem of the coxib pharmacophore rather than any idiosyncratic property of one drug call for development of novel inhibitors of the COX-2 enzyme of natural origin and different chemical structure.

Silybum marianum (milk thistle) is an extensively used herb that offers protection against liver injury, wherein the main bioactive ingredient of the herb known as silymarin includes flavonolignans (silybin A/B, isosilybin A/B, silychristin, and silydianin), and flavones (taxifolin and quercetin) [14,15]. Silymarin has exhibited selective inhibition of COX-2 through NF-κB suppression and inhibition of oxidative stress in endothelial and hepatic systems, including COX-2 inhibition caused by tacrolimus in human umbilical vein endothelial cells [15,16]. Although these studies have established the suppression of transcription of COX-2, there is still

uncertainty regarding the capacity of individual plant extracts to provide isoform-specific, direct inhibition of the enzyme active site, similar to the coxibs drugs available in clinical practice or if these compounds have pharmacokinetic properties for oral delivery.

The approach of computer-aided drug design (CADD), which combines molecular docking analysis with ADMET/toxicity predictions, provides an answerable path to this question. Through network pharmacology and docking analyses, COX-2 has emerged as an important hub in the anti-inflammatory action of complex plant combinations by mapping the interaction network of the plant components with targets such as PTGS2, TNF, IL-6, MAPK1, AKT1, and related NF-κB pathway nodes [17,18]. Combining these analyses with the ADMET screening tools (SwissADME, pkCSM, ADMETLab) allows identification of candidate molecules with better absorption and reduced hepatic/cardiotoxic potential compared to the current NSAIDs [19,20], while simultaneous docking/simulation studies on both synthetic and natural COX-2 ligands help develop structure-selectivity relationships for NSAID analogs [21,22].

A binding pose created by a single docking run, on the other hand, cannot be considered a strong piece of evidence unless its reproducibility is verified independently; a plausible but not a reproducible pose can lead to incorrect interpretation of the interaction. The current research work thus uses docking binding energies along with replicable RMSD reproducibility verification, but not complete molecular dynamics, as the appropriate method of measuring pose reproducibility in a 23 compound comparison screening using S. marianum ligand library against human COX-2 (PDB: 3LN1) and COX-1 counter screening, compared with clinically available NSAIDs/ coxibs in order to find candidates that possess high isoform selectivity, good ADMET properties, and acceptable toxicity as leads for the synthesis of anti-inflammatory drugs.

Material and methods

The methodological flow chart of the research paper is shown in Figure 1.

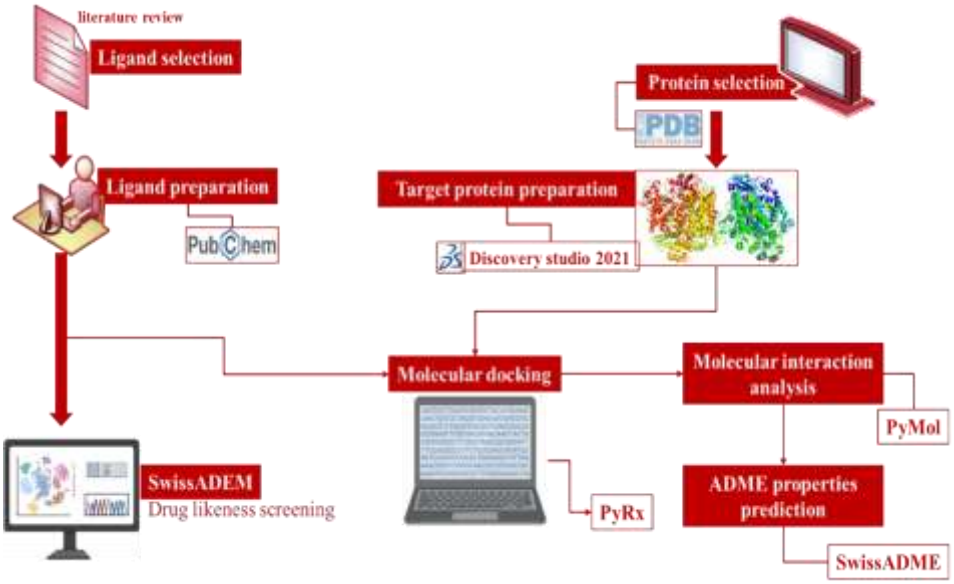

Figure (1): Schematic diagram depicting the workflow for ligand selection, molecular docking, and ADME property prediction.

Protein and Ligand Preparation

The crystal structure of the COX-2 enzyme (PDB ID: 3LN1) and the COX-1 template for the counter-screening (PDB ID: 7JXT) were obtained from the RCSB Protein Data Bank and subjected to processing in BIOVIA Discovery Studio 2021 through deletion of crystallographic water molecules and the co-crystallized ligand. The phytochemical library of the constituent compounds of S. marianum was compiled based on data from ethnopharmacological literature [23,24] and consisted of the following compounds: isosilybin A, isosilybin B, silychristin, silydianin, silybin A, silybin B, quercetin, taxifolin, and α-curcumene, as well as other constituents (retinal, linoleic acid, ethyl cholate). 3D structures were extracted from PubChem and energy-minimized. In addition, nine NSAIDs/COX-1B inhibitors (celecoxib, etodolac, etoricoxib, ibuprofen, lumiracoxib, meloxicam, nabumetone, parecoxib, and rofecoxib), along with valdecoxib and polmacoxib as comparators, were constructed in ChemDraw and converted to 3D SDF format.

Molecular Docking Protocol

Docking was done using PyRx 0.8 (AutoDock Vina) on an active site grid box of COX-2 (center X 28.09, Y -21.27, Z -16.71; size 38.89 x 36.25 x 39.58 Å) and a COX-1 counter-screen grid box (22 x 22 x 22 Å; center X 27.59, Y 157.23, Z 3.80), both having exhaustiveness = 8. Visualization of interactions after docking were done using BIOVIA Discovery Studio and PyMOL. The reproducibility of each pose generated through molecular docking was evaluated using PyMOL to superimpose two replicate docking simulations per ligand-isoform pair and compute the Root Mean Square Deviation (RMSD), where RMSD ≤ 2.0 Å was taken as evidence of convergence, while RMSD up to 3.0 Å was tolerable for large, flexible flavonolignan-class ligands.

Selectivity Index and Statistical Standardization

The selectivity index was calculated as SI = (ΔG COX-2) / (ΔG COX-1), where SI > 1.0 indicates COX-2 preferential binding and SI < 1.0 denotes COX-1 selectivity. In order to allow for independent comparison irrespective of distribution in the docked library, the Z-scores of COX-1 ΔG, COX-2 ΔG, and SI were calculated and represented on a hierarchical heatmap created in SRplot [25].

ADMET and Toxicity Prediction

Predicted physicochemical descriptors include molecular weight, LogP, TPSA, LogS, hydrogen bond donors/receptors. Predicted descriptors regarding drug-likeness and absorption: Lipinski and Veber compliance, intestinal absorption, BBB permeability, P-glycoprotein substrate, skin permeability (Log Kp), and bioavailability score were calculated by using SwissADME. Inhibition of cytochrome P450 enzymes (CYP1A2, CYP2C9, CYP2C19, CYP2D6, CYP3A4) was estimated on the same platform. Acute oral toxicity (LD_{50}, GHS classification) was predicted from canonical PubChem SMILES by ProTox-II.

Results and discussion

Isoform Selectivity and Docking Validation

Reference validation confirmed the docking protocol's reliability: celecoxib bound COX-2 with ΔG = −12.1 kcal/mol versus −9.5 kcal/mol for COX-1 (SI = 1.27), consistent with its established clinical selectivity (Table 1). Among the phytoconstituents, the flavonolignan cluster (isosilybin A/B, silychristin, silydianin, silybin A/B) uniformly favored COX-1 (SI 0.81–0.89; COX-1 ΔG −10.2 to −10.9 kcal/mol), whereas the smaller flavonols quercetin and taxifolin inverted this preference, achieving SI values of 1.10 and 1.13, respectively — placing them in the same selectivity range as the clinical coxibs (celecoxib, rofecoxib, etoricoxib, valdecoxib, lumiracoxib; SI 1.13–1.27; Table 1).

Critically, this COX-2 preference did not arise from reduced COX-1 affinity (quercetin/taxifolin COX-1 ΔG −8.7 to −8.8 kcal/mol, near the cohort mean) but from enhanced absolute COX-2 binding (−9.7 to −9.8 kcal/mol). Z-score clustering (Figure 2) confirmed this mechanistic distinction: quercetin, taxifolin, celecoxib, and rofecoxib co-clustered on near-neutral Z-COX-1 and strongly negative Z-COX-2 scores, indicating that selectivity is driven by superior COX-2 engagement rather than COX-1 avoidance. α-Curcumene, despite modest absolute affinities (COX-1 ΔG −6.1; COX-2 ΔG −7.9 kcal/mol), returned the highest standardized selectivity value in the dataset (Z-SI = 1.85) through the converse mechanism — comparatively weak COX-1 binding — clustering instead with etoricoxib, valdecoxib, lumiracoxib, and nabumetone.

Isoform Selectivity and Docking Validation

Reference validation confirmed the docking protocol's reliability: celecoxib bound COX-2 with ΔG = −12.1 kcal/mol versus −9.5 kcal/mol for COX-1 (SI = 1.27), consistent with its established clinical selectivity (Table 1). Among the phytoconstituents, the flavonolignan cluster (isosilybin A/B, silychristin, silydianin, silybin A/B) uniformly favored COX-1 (SI 0.81–0.89; COX-1 ΔG −10.2 to −10.9 kcal/mol), whereas the smaller flavonols quercetin and taxifolin inverted this preference, achieving SI values of 1.10 and 1.13, respectively — placing them in the same selectivity range as the clinical coxibs (celecoxib, rofecoxib, etoricoxib, valdecoxib, lumiracoxib; SI 1.13–1.27; Table 1).

Critically, this COX-2 preference did not arise from reduced COX-1 affinity (quercetin/taxifolin COX-1 ΔG −8.7 to −8.8 kcal/mol, near the cohort mean) but from enhanced absolute COX-2 binding (−9.7 to −9.8 kcal/mol). The Z-score clustering analysis (Figure 2) further supported this mechanistic differentiation, with quercetin, taxifolin, celecoxib, and rofecoxib clustering in a near-neutral Z-COX-1 score and strongly negative Z-COX-2 score, confirming that the mechanism behind selectivity involves the ability to interact preferentially with COX-2 over COX-1. Interestingly, α-curcumene, while having relatively moderate binding affinities to both COX isoforms (ΔG COX-1 = -6.1; ΔG COX-2 = -7.9 kcal/mol), yielded the maximum standardized

selectivity score (Z-SI = 1.85) in the current study through the opposite approach of weaker binding to COX-1 clustering with etoricoxib, valdecoxib, lumiracoxib, and nabumetone. The docking pose reproducibility analysis using the RMSD metric (Table 1) showed good convergence of poses across replicate runs (RMSD < 2.0 Å in most cases), with relatively higher RMSD values seen for larger ligands with flexible conformations such as isosilybin A (2.665 Å, COX-1) and polmacoxib (2.407 Å, COX-2), both falling within the range of ≤3.0 Å for structurally complex and flexible ligands.

Table 1. Docking binding energies, RMSD, and Selectivity Index for *S. marianum* phytoconstituents versus reference agents against human COX-1 and COX-2.

Compound	Group	COX-1 ΔG (kcal/mol)	RMSD (Å)	COX-2 ΔG (kcal/mol)	RMSD (Å)	SI[a]
Isosilybin A	Phytoconstituent	−10.9	2.665	−9.6	2.083	0.88
Isosilybin B	Phytoconstituent	−10.8	1.735	−8.8	0.838	0.81
Silychristin	Phytoconstituent	−10.5	0.592	−9.3	1.880	0.89
Silydianin	Phytoconstituent	−10.4	1.083	−8.8	1.293	0.85
Silybin A	Phytoconstituent	−10.2	1.106	−9.1	1.138	0.89
Silybin B	Phytoconstituent	−10.3	1.113	−9.0	1.612	0.87
Quercetin	Phytoconstituent	−8.8	0.517	−9.7	0.788	1.10
Taxifolin	Phytoconstituent	−8.7	0.712	−9.8	0.799	1.13
α-Curcumene	Phytoconstituent	−6.1	1.088	−7.9	0.976	1.30
Retinal	Phytoconstituent	−7.8	1.142	−6.4	1.442	0.82
Linoleic acid	Phytoconstituent	−6.4	1.062	−6.2	1.014	0.97
Ethyl cholate	Phytoconstituent	−8.8	0.665	−7.5	0.982	0.85
Celecoxib	Reference	−9.5	0.763	−12.1	1.571	1.27
Rofecoxib	Reference	−8.8	0.819	−10.7	1.054	1.22
Etoricoxib	Reference	−7.3	0.450	−8.5	0.906	1.16
Valdecoxib	Reference	−7.6	0.579	−9.1	1.215	1.20
Lumiracoxib	Reference	−8.0	0.953	−9.0	0.896	1.13
Parecoxib	Reference	−9.1	1.323	−8.8	1.457	0.97
Polmacoxib	Reference	−8.8	0.771	−8.7	2.407	0.99
Meloxicam	Reference	−8.5	0.570	−7.4	0.370	0.87
Etodolac	Reference	−8.4	0.377	−7.2	0.563	0.86
Nabumetone	Reference	−7.5	0.647	−8.3	0.925	1.11
Ibuprofen	Reference	−7.4	0.733	−7.7	0.578	1.04

[a] SI = (ΔG COX-2) / (ΔG COX-1); SI > 1.0 indicates COX-2 preference, SI < 1.0 indicates COX-1 preference.

A third cluster identified by the hierarchical heatmap clustering represented an additional classification beyond the quercetin/taxifolin-coxib and COX-1-preferential flavonolignan clusters: α-curcumene clustered alongside etoricoxib, valdecoxib, lumiracoxib, and nabumetone on a common signature of relatively low COX-1 preference along with moderate COX-2 affinity. This represents a different mechanistic basis for positive selectivity compared to quercetin/ taxifolin/ celecoxib/ rofecoxib, and it is also worth noting that this second cluster includes the two coxibs with the worst post-market safety profiles (rofecoxib withdrawn from the market due to adverse effects, etoricoxib's dermatological side effect signal), prompting the question – one that goes well beyond docking alone – if avoidance of COX-1 selectivity brings a specific CV risk profile compared to potent COX-2 selectivity. The flavonolignan cluster was, on the other hand, statistically undistinguishable from a COX-1-preferential profile on both Z-COX-1 and Z-SI axes, indicating that the natural form of these compounds is unlikely to act as selective COX-2 inhibitors in any formulation.

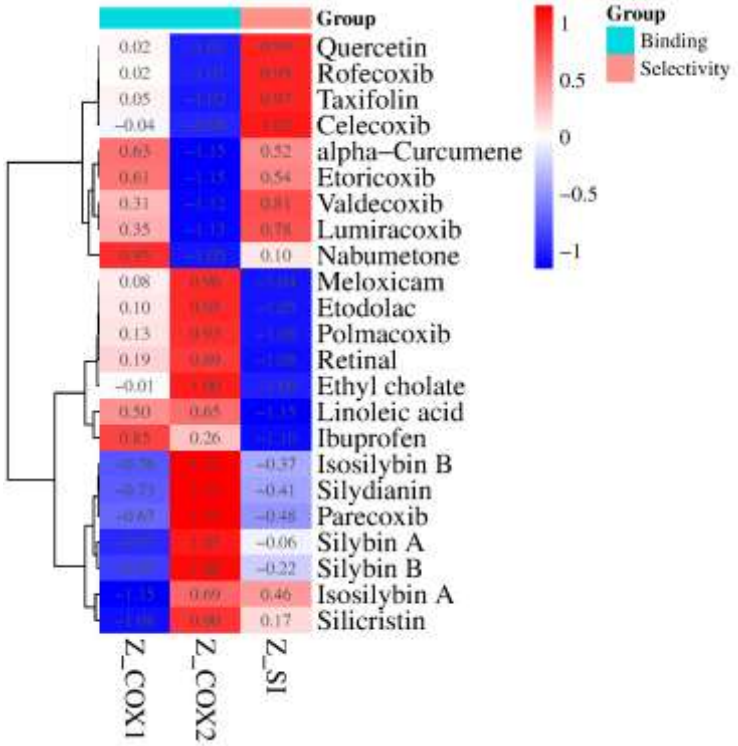

Figure 2. Heatmap showing hierarchically clustered standardized Z-scores of COX-1 binding affinity, COX-2 binding affinity and Selectivity Index of all 23 docked compounds, where the columns indicate the type of binding-affinity or selectivity index being displayed.

Active-Site Interaction Analysis

Inspection of the active site cavity of the COX-2 enzyme (Figure 3) revealed Val509 to be a common hydrophobic anchor involved in interactions with celecoxib, quercetin, and α-curcumene through Pi-Sigma/Pi-Alkyl interactions, whereas the polar interaction was made with Ser339 by only celecoxib and quercetin. The hydrogen bonding with Ser339 of quercetin, along with hydrophobic stabilisation from Val509 and Leu338, mimics the polar-hydrophobic interaction pattern of the sulfonamide/trifluoromethyl-phenyl pharmacophoric group of celecoxib. The interaction of taxifolin, on the other hand, is with a different set of residues located at the N-terminus (Asn24, Asn28, Cys26) and a pi-cation interaction with Arg29, attributed to the saturation of the C2-C3 bond resulting in alteration of C-ring geometry compared with quercetin, which directs it towards a more peripheral location within the active site channel. The interactions of α-curcumene, which does not have any hydrogen donor/acceptors, were made exclusively through alkyl/pi-alkyl interaction with Val509, Met508, His75, and Trp373, which is indicative of a non-competitive mode of binding.

Based on the consistent engagement of Val509 between the three most selective COX-2 ligands among all natural ligands studied here, the Val509 site would seem to be an attractive anchor point for the next generation of quercetin-scaffold semi-synthetics, although the N-terminal engagement unique to taxifolin indicates another potential avenue for achieving selectivity through structural modification. Structure-activity considerations suggest that the comparative study of quercetin versus taxifolin is enlightening precisely because the only difference between the two molecules is one chemical structure element: saturation of the C2-C3 bond within the C-ring of taxifolin, which causes the loss of planarity of this ring and therefore the change in the preferred subpocket of taxifolin binding without affecting the binding energy and selectivity index. Therefore, it seems that C-ring saturation, rather than the size or polarity of the molecule, is an adjustable factor that allows you to guide the interaction of flavonoids either in the hybrid pocket with Ser339/Val509 or in the N-terminal polar cluster.

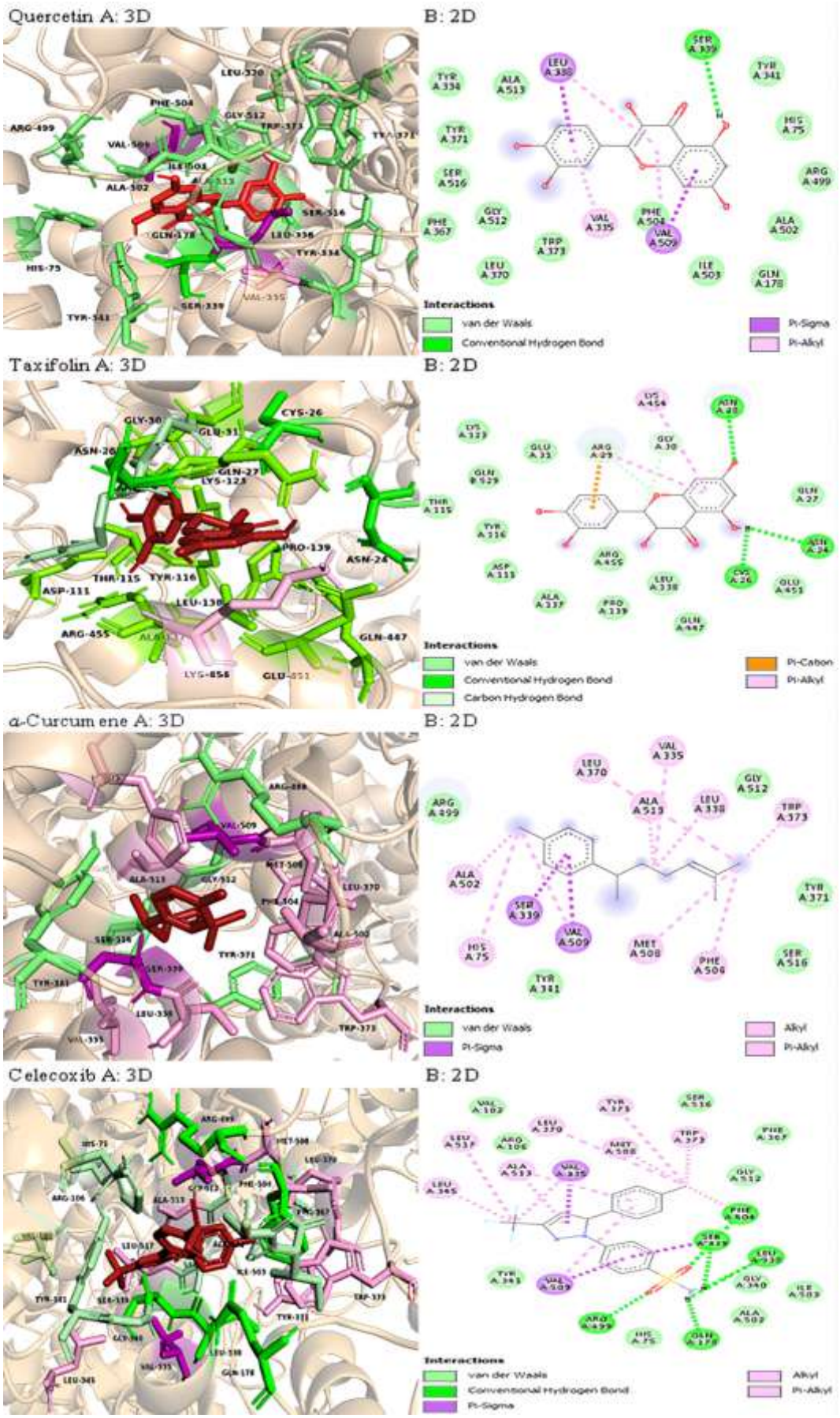

Figure (3): Molecular docking analysis and intermolecular interaction profiles of Quercetin, Taxifolin, α-Curcumene, and Celecoxib within the COX-2 catalytic site (PDB ID: 3LN1).

The TPSA Barrier: Physicochemical Basis for Differential Bioavailability

Contrast with physicochemical analysis (see Table 2), explains why nearly all constituents of S. marianum meet Lipinski's rule of five (molecular weight < 500 Da, no violations of the rule), yet only quercetin and taxifolin show high GI absorption (Table 3). Flavonolignan group (molecular weight 482.44 g/mol) shows TPSA ranging 155–166 Å² and 5–6 hydrogen bond donors, which are above Veber's ≤140 Å² oral bioavailability limit, but LogP (1.97–3.10) and aqueous solubility (LogS ≈ −3.4 to −4.1) are comparable with that of reference NSAIDs. This mismatch between the presence of adequate lipophilicity/solubility and the absence of predicted high absorption suggests desolvation penalty as the major factor limiting permeability. Indeed, this is in line with previous pharmacokinetic characterization of silymarin flavonolignans as poorly bioavailable despite adequate solubility [26], [27]. However, both quercetin (TPSA 131.36 Å²; MW 302.24) and taxifolin (TPSA 127.45 Å²; MW 304.25) are below this permeability limit, making their pharmacokinetic profile more similar to that of synthetic coxibs such as celecoxib (TPSA 86.36 Å²) and providing an explanation for their better expected GI absorption properties. No constituent of the S. marianum extracts was found capable of crossing the blood-brain barrier, thereby restricting their activity to peripheral tissues, which may be an acceptable trade-off for the sake of hepato-protective action of silymarin, though making the central analgesic effect impossible in comparison with BBB-permeable NSAIDs such as etodolac, ibuprofen, lumiracoxib, nabumetone and rofecoxib.

Table 2. Comparative physicochemical profiling of phytoconstituents and reference drugs.

Compound	Group	Formula	MW (g/mol)	LogP	TPSA (Å²)	LogS	HBA	HBD
Isosilybin A	Phytoconstituent	$C_{25}H_{22}O_{10}$	482.44	2.73	155.14	−4.14	10	5
Isosilybin B	Phytoconstituent	$C_{25}H_{22}O_{10}$	482.44	3.10	155.14	−4.14	10	5
Silychristin	Phytoconstituent	$C_{25}H_{22}O_{10}$	482.44	2.31	166.14	−3.93	10	6
Silydianin	Phytoconstituent	$C_{25}H_{22}O_{10}$	482.44	1.97	162.98	−3.39	10	5
Silybin A	Phytoconstituent	$C_{25}H_{22}O_{10}$	482.44	2.40	155.14	−4.14	10	5
Silybin B	Phytoconstituent	$C_{25}H_{22}O_{10}$	482.44	2.82	155.14	−4.14	10	5
Quercetin	Phytoconstituent	$C_{15}H_{10}O_7$	302.24	1.63	131.36	−3.16	7	5
Taxifolin	Phytoconstituent	$C_{15}H_{12}O_7$	304.25	0.71	127.45	−2.66	7	5
α-Curcumene	Phytoconstituent	$C_{15}H_{22}$	202.34	3.50	0.00	−4.52	0	0
Celecoxib	Reference	$C_{17}H_{14}F_3N_3O_2S$	381.37	2.56	86.36	−4.57	3	1
Etodolac	Reference	$C_{16}H_{21}NO$	243.34	2.23	25.02	−3.45	2	3
Etoricoxib	Reference	$C_{18}H_{15}ClN_2O_2S$	358.84	2.75	68.30	−4.53	2	0
Ibuprofen	Reference	$C_{13}H_{18}O_2$	206.20	2.17	37.30	−3.36	1	2
Lumiracoxib	Reference	$C_{15}H_{13}ClFNO_2$	293.72	2.38	49.33	−4.46	2	3
Meloxicam	Reference	$C_{14}H_{13}N_3O_4S_2$	351.40	1.74	136.22	−4.34	2	5
Nabumetone	Reference	$C_{15}H_{16}O_2$	228.29	2.74	26.30	−3.37	0	2
Parecoxib	Reference	$C_{19}H_{18}N_2O_4S$	370.42	2.28	97.65	−4.28	1	5
Rofecoxib	Reference	$C_{17}H_{14}O_4S$	314.36	2.13	68.82	−3.42	0	4

However, in relation to classifying silydianin as a flavonolignan and etodolac as an NSAID as a part of the set of known P-gp substrates, one can note that these drugs have the isolated property of a possibility of efflux-limited

intracellular accumulation.The permeability problem for flavonolignans, viewed not as a dead-end for the molecule but as a formulation issue, is perfectly consistent with, not in conflict with, the positive values of both LogP and LogS properties of flavonolignans (Table 2). The barrier is specifically a desolvation/permeability barrier, not a solubility barrier, and the latter is a much harder one to deal with in drug design. Formulations that have been described for structurally similar polyphenols (lipid formulations, liposomes, permeation enhancers, and hydrogen bond donor masking prodrugs), would allow addressing this particular barrier without altering the core pharmacophore that engages with the targets, thus giving hope of recovery of the COX-binding properties of flavonolignans in an oral formulation [23].

Table 3. Comparative predicted pharmacokinetic properties.

Compound	Group	GI Absorption	BBB Permeant	P-gp Substrate	Log Kp	Bioavailability Score
Isosilybin A	Phytoconstituent	Low	No	No	−7.89	0.55
Isosilybin B	Phytoconstituent	Low	No	No	−7.89	0.55
Silychristin	Phytoconstituent	Low	No	No	−8.14	0.55
Silydianin	Phytoconstituent	Low	No	Yes	−8.67	0.55
Silybin A	Phytoconstituent	Low	No	No	−7.89	0.55
Silybin B	Phytoconstituent	Low	No	No	−7.89	0.55
Quercetin	Phytoconstituent	High	No	No	−7.05	0.55
Taxifolin	Phytoconstituent	High	No	No	−7.48	0.55
α-Curcumene	Phytoconstituent	Low	No	No	−3.71	0.55
Celecoxib	Reference	High	No	No	−6.21	0.55
Etodolac	Reference	High	Yes	Yes	−6.06	0.85
Etoricoxib	Reference	High	No	No	−6.12	0.55
Ibuprofen	Reference	High	Yes	No	−5.07	0.85
Lumiracoxib	Reference	High	Yes	No	−5.14	0.85
Meloxicam	Reference	High	No	No	−6.01	0.56
Nabumetone	Reference	High	Yes	No	−5.51	0.55
Parecoxib	Reference	High	No	No	−6.24	0.55
Rofecoxib	Reference	High	Yes	No	−6.61	0.55

Metabolic Interaction Potential and Herb–Drug Interaction Risk

Based on the CYP450 inhibition profiling data (Table 4), CYP3A4 was identified as the dominant CYP inhibitor isoform among flavonolignans (silybin A/B, isosilybin A, silychristin), which is justified by the ability of silymarin to affect the process of drug metabolism, since CYP3A4 metabolizes about 50% of commercial drugs. The broadest profile of inhibition activity was demonstrated by quercetin (CYP3A4, CYP2D6, CYP1A2), overlapping directly with the etoricoxib profile (CYP3A4, CYP1A2). Accordingly, a concomitant use of quercetin-rich milk thistle preparation together with etoricoxib would be capable of decreasing their clearance, increasing gastrointestinal or cardiovascular risks associated with their elevated levels. According to the computational modeling, taxifolin, isosilybin B, and silydianin were considered to be CYP-inert, thus,

taxifolin possessed a high degree of selectivity and low risk of interactions. The reference group of NSAIDs had a higher degree of inhibition (CYP1A2/CYP2C19 inhibited by 6 out of 9 drugs), except for ibuprofen that was predicted to be CYP-inert for all five isoforms.

Apart from being clinically relevant in view of the etoricoxib/quercetin combination, this interaction is relevant also from the pharmacokinetics potentiation point of view, since any combinations of patients receiving milk thistle extract to protect their liver in conjunction with some NSAIDs metabolized via CYP3A4 or CYP2C9 (those would be celecoxib, lumiracoxib, meloxicam, parecoxib, and rofecoxib according to current data set) are potentially susceptible to the same kind of interaction, as the silymarin extract is normally available over-the-counter as a hepatoprotector, not as a pharmacologically active medication in combination. In this situation, the fact that taxifolin is CYP-inert is one more property to take into account regardless of COX-2 specificity.

Table 4. Predicted Cytochrome P450 (CYP450) inhibition profile.

Compound	Group	CYP1A2	CYP2C9	CYP2C19	CYP2D6	CYP3A4
Isosilybin A	Phytoconstituent	Yes	No	No	No	No
Isosilybin B	Phytoconstituent	No	No	No	No	No
Silychristin	Phytoconstituent	Yes	No	No	No	No
Silydianin	Phytoconstituent	No	No	No	No	No
Silybin A	Phytoconstituent	Yes	No	No	No	No
Silybin B	Phytoconstituent	Yes	No	No	No	No
Quercetin	Phytoconstituent	Yes	No	Yes	No	Yes
Taxifolin	Phytoconstituent	No	No	No	No	No
α-Curcumene	Phytoconstituent	No	No	Yes	No	No
Celecoxib	Reference	Yes	Yes	No	No	No
Etodolac	Reference	Yes	No	Yes	Yes	No
Etoricoxib	Reference	Yes	No	Yes	Yes	Yes
Ibuprofen	Reference	No	No	No	No	No
Lumiracoxib	Reference	Yes	Yes	Yes	Yes	No
Meloxicam	Reference	No	Yes	No	No	Yes
Nabumetone	Reference	Yes	No	Yes	Yes	No
Parecoxib	Reference	No	Yes	Yes	No	Yes
Rofecoxib	Reference	Yes	Yes	Yes	No	No

Predicted Acute Toxicity

The ProTox-II predictions of Table 5 indicate that most of the components of silymarin fall into the practically non-toxic category (LD_{50} 2000–10,000 mg/kg; median 2000 mg/kg), which is higher than the median value of the reference-NSAID dataset (2240 mg/kg). The only exception is quercetin, whose predicted LD_{50} is equal to 159 mg/kg. This value significantly differs from the in vivo measurements indicating LD_{50} of dietary quercetin

above 2000 mg/kg [28], a finding consistent with the known tendency of in silico toxicity models to overestimate the acute toxicity of polyphenolic flavonoids [29], [30]. Such an uncertainty should be considered explicitly while evaluating the developability potential of quercetin. In contrast, the LD_{50} values for silibinin containing products (LD_{50} 2000-5000 mg/kg in rodents; [31, 32]) are consistent with the in silico predicted LD_{50} of 2000 mg/kg for flavonolignans, thus indicating the accuracy of this part of the toxicity database. According to GHS acute toxicity criteria, an LD_{50} of around 2000 mg/kg puts these components right on the verge between Category 5 (the least hazardous one) and Category 4, while the estimated value of 159 mg/kg for quercetin would place it into Category 3 (quite hazardous). Such a significant discrepancy between categories (from low concern to moderate) may have a notable impact on a risk assessment, which is exactly the reason why this deviation from the results obtained in experiments (LD_{50} > 2000 mg/kg; [28]) should be clarified.

Table 5. Predicted median lethal dose (LD_{50}, mg/kg) and toxicological classification.

Compound	Group	Predicted LD_{50} (mg/kg)
Isosilybin A	Phytoconstituent	2000
Isosilybin B	Phytoconstituent	2000
Silychristin	Phytoconstituent	2000
Silydianin	Phytoconstituent	10,000
Silybin A	Phytoconstituent	2000
Silybin B	Phytoconstituent	2000
Quercetin	Phytoconstituent	159
Taxifolin	Phytoconstituent	2000
α-Curcumene	Phytoconstituent	2000
Celecoxib	Reference	1400
Etodolac	Reference	2200
Etoricoxib	Reference	2500
Ibuprofen	Reference	299
Lumiracoxib	Reference	56
Meloxicam	Reference	136
Nabumetone	Reference	3880
Parecoxib	Reference	3000
Polmacoxib	Reference	8000
Rofecoxib	Reference	2240
Valdecoxib	Reference	6081

Conclusion

The in silico screening has determined taxifolin and quercetin to be the Silybum marianum flavonoids exhibiting structural similarity and pharmacokinetic potential toward selective inhibition of cyclooxygenase-2 activity, targeting the Ser339/ Val509 recognition site also present in celecoxib, thus attaining selectivity ratio comparable with that of the coxib class. Based on the physicochemical analysis, the low bioavailability of the large flavonolignans is due to a desolvation penalty induced by TPSA rather than insolubility, providing a scientific explanation of possible value for the development of pro-drugs or nanomaterials aimed at overcoming this barrier in order to capitalize on the potential for target recognition based on favorable lipophilicity.

Considering that the results have been obtained computationally, including an assessment of quercetin cytotoxicity inconsistent with experimental data, such information should be considered as a structural basis for further studies rather than a treatment recommendation. In vitro assays for cyclooxygenase inhibition and free energy refinement (such as MM/GBSA and free-energy perturbation methods) coupled with validation in vivo of pharmacodynamics and toxicology would be required in order to evaluate the potential of either molecule or derivatives of quercetin as COX-2 inhibitors. Under these constraints, the main contribution of the study can be described as a structural and physicochemical basis — based on the conserved Ser339/Val509 motif and TPSA-permeability threshold — for the selection of precisely two minor silymarin components and not its well-known flavonolignans as promising candidates for COX-2 inhibitor design.

References

[1] Khalil, N. A., Ahmed, E. M., Tharwat, T., & Mahmoud, Z. (2024). NSAIDs between past and present; a long journey towards an ideal COX-2 inhibitor lead. *RSC advances*, *14*(42), 30647–30661.

[2] Chen, L., Deng, H., Cui, H., Fang, J., Zuo, Z., Deng, J., ... & Zhao, L. (2018). Inflammatory responses and inflammation-associated diseases in organs. *Oncotarget*, 9(7), 7204-7218.

[3] Chavda, V. P., Feehan, J., & Apostolopoulos, V. (2024). Inflammation: The Cause of All Diseases. *Cells*, *13*(22), 1906.

[4] Jin K, Qian C, Lin J and Liu B (2023) Cyclooxygenase-2-Prostaglandin E2 pathway: A key player in tumor-associated immune cells. Front. Oncol. 13:1099811.

[5] Surai, P. F., Surai, A., & Earle-Payne, K. (2024). Silymarin and Inflammation: Food for Thoughts. *Antioxidants (Basel, Switzerland)*, *13*(1), 98.

[6] Lee, H., Jeong, G. H., Lee, S. S., Lee, K. B., Park, S., Kim, T. H., Bai, H. W., & Chung, B. Y. (2025). Rosmarinosin A Inhibits Inflammatory Response in Lipopolysaccharide-Induced RAW 264.7 Macrophages via Suppressing NF-κB and MAPK Signaling Pathway. *Molecules (Basel, Switzerland)*, *30*(18), 3752.

[7] Alqudah, A., Barakat, M., Alzaghari, L. F., Qnais, E., Gammoh, O., Alqudah, M., Aljabali, A. A., & Shilbayeh, S. A. R. (2024). Mechanistic Insights into Isorhamnetin: Targeting MAPK and NF-κB Pathways to Mitigate LPS-Induced Inflammation. *Current molecular pharmacology*, *17*, e18761429385248.

[8] Li, Zhendong, Man Li, Zhi Fang, and Haijun Wang. (2025). "Immunological Mechanisms and Therapeutic Strategies in Cerebral Ischemia–Reperfusion Injury: From Inflammatory Response to Neurorepair" *International Journal of Molecular Sciences* 26, no. 17: 8336.

[9] Simancas-Racines, D., Jiménez-Flores, E., Montalvan, M., Horowitz, R., Araujo, V., & Reytor-González, C. (2026). Endometriosis as a Systemic and Complex Disease: Toward Phenotype-Based Classification and Personalized Therapy. *International journal of molecular sciences*, *27*(2), 908.

[10] Chahal, S., Rani, P., Kiran, Sindhu, J., Joshi, G., Ganesan, A., Kalyaanamoorthy, S., Mayank, Kumar, P., Singh, R., & Negi, A. (2023). Design and Development of COX-II Inhibitors: Current Scenario and Future Perspective. *ACS omega*, *8*(20), 17446–17498.

[11] Mathe, A., & Karlapudi, A. P. (2025). Computational and experimental evaluation of a dual COX inhibitor: Insights from DFT, molecular simulations, and in-vitro validation. *Letters in Drug Design & Discovery*, *22*(2), Article 100009. ISSN 1570-1808.

[12] Sohail, R., Mathew, M., Patel, K. K., Reddy, S. A., Haider, Z., Naria, M., Habib, A., Abdin, Z. U., Chaudhry, W. R., & Akbar, A. (2023). Effects of non-steroidal anti-inflammatory drugs (NSAIDs) and gastroprotective NSAIDs on the gastrointestinal tract: A narrative review. *Cureus*, *15*(4), e37080.

[13] Ansari, M. A., & Kumar, A. (2025). Etoricoxib and its hidden risks: a case-based review of dermatological, hematological, and cardiovascular complications. *EXCLI journal*, *24*, 1295–1334.

[14] Muchiri, R. N.; van Breemen, R. B. Chemical Standardization of Milk Thistle (*Silybum marianum* L.) Extract Using UHPLC-MS/MS and the Method of Standard Addition. *J. Am. Soc. Mass Spectrom.* 2024, *35*, 1726−1732.

[15] Jaffar, H. M., Al-Asmari, F., Khan, F. A., Rahim, M. A., & Zongo, E. (2024). Silymarin: Unveiling its pharmacological spectrum and therapeutic potential in liver diseases—A comprehensive narrative review. *Food Science & Nutrition*, 12(5), 3097–3111.

[16] Chen, Y. C., Chang, K. T., Chen, P. M., & Chen, H. H. (2025). Silymarin Ameliorates Tacrolimus-induced Inflammation in Human Umbilical Vein Endothelial Cells. *In vivo (Athens, Greece)*, *39*(5), 2617–2628.

[17] Ren, J., Ding, Y., Li, S., & Lei, M. (2023). Predicting the anti-inflammatory mechanism of Radix Astragali using network pharmacology and molecular docking. *Medicine*, *102*(35), e34945.

[18] Merecz-Sadowska, A., Sadowski, A., Zielińska-Bliźniewska, H., Zajdel, K., & Zajdel, R. (2025). Network Pharmacology as a Tool to Investigate the Antioxidant and Anti-Inflammatory Potential of Plant Secondary Metabolites—A Review and Perspectives. *International Journal of Molecular Sciences*, *26*(14), 6678.

[19] Yousafzai, U., Najia Javed, Ali, S. L., Awais Ali, & Amir Hamza. (2025). Computer-aided Discovery of Novel COX-2 Inhibitors for Anti-inflammatory Therapy Using Pharmacophore Modelling, Molecular Docking, ADMET, and Virtual Screening. *Advances in Modern Biomedicine*, *1*(4), 25-38.

[20] Bettadj, F. Z. Y., & Benchouk, W. (2023). Computer-aided analysis for identification of novel analogues of ketoprofen based on molecular docking, ADMET, drug-likeness and DFT studies for the treatment of inflammation. *Journal of biomolecular structure & dynamics*, *41*(19), 9915–9930.

[21] Swain, G., Jain, S., Gupta, A., Pal, D., & Kumar, N. (2025). Investigation of Novel Etoricoxib Analogues as Potential COX-II Inhibitors through a Bioisosteric Strategy, ADMET Evaluations, Docking Studies, and Molecular Dynamics Simulations. *Current computer-aided drug design*.

[22] Xiang, C., Liao, Y., Chen, Z., Xiao, B., Zhao, Z., Li, A., Xia, Y., Wang, P., Li, H., & Xiao, T. (2022). Network Pharmacology and Molecular Docking to Elucidate the Potential Mechanism of Ligusticum Chuanxiong Against Osteoarthritis. *Frontiers in pharmacology*, *13*, 854215.

[23] Makouie, S., Bryś, J., Małajowicz, J., Koczoń, P., Siol, M., Palani, B. K., Bryś, A., Obranović, M., Mikolčević, S., & Gruczyńska-Sękowska, E. (2024). A comprehensive review of silymarin extraction and liposomal encapsulation techniques for potential applications in food. *Applied Sciences*, *14*(18), 8477.

[24] Gaber, H.H., Sedki, A.G., El Sherbiny, W.A. and Elgendy, E.M. (2022) Biological in Vitro and in Vivo Studies of the Milk Thistle Seed Oil. Food and Nutrition Sciences, 13, 1015-1035.

[25] Tang D, Chen M, Huang X, Zhang G, Zeng L, Zhang G, Wu S, Wang Y. SRplot: A free online platform for data visualization and graphing. *PLoS One*. 2023;18(11):e0294236.

[26] Tvrdý, V., Pourová, J., Jirkovský, E., Křen, V., Valentová, K., & Mladěnka, P. (2021). Systematic review of pharmacokinetics and potential pharmacokinetic interactions of flavonolignans from silymarin. *Medicinal Research Reviews, 41,* 2195 - 2246.

[27] Ahmad, S., Khan, J. A., Kausar, T. N., Mahnashi, M. H., Alasiri, A., Alqahtani, A. A., Alqahtani, T. S., Walbi, I. A., Alshehri, O. M., Elnoubi, O. A., Mahmood, F., & Sadiq, A. (2023). Preparation, Characterization and Evaluation of Flavonolignan Silymarin Effervescent Floating Matrix Tablets for Enhanced Oral Bioavailability. *Molecules (Basel, Switzerland)*, *28*(6), 2606.

[28] Ortiz-Andrade, R., Araujo-León, J. A., Sánchez-Recillas, A., Navarrete-Vazquez, G., González-Sánchez, A. A., Hidalgo-Figueroa, S., Alonso-Castro, Á. J., Aranda-González, I., Hernández-Núñez, E., Coral-Martínez, T. I., Sánchez-Salgado, J. C., Yáñez-Pérez, V., & Lucio-Garcia, M. A. (2020). Toxicological Screening of Four Bioactive Citroflavonoids: In Vitro, In Vivo, and In Silico Approaches. *Molecules*, *25*(24), 5959.

[29] Noga, M., Michalska, A., & Jurowski, K. (2024). The prediction of acute toxicity (LD_{50}) for organophosphorus-based chemical warfare agents (V-series) using toxicology in silico methods. *Archives of toxicology*, *98*(1), 267–275.

[30] Bitew, M., Desalegn, T., Demissie, T. B., Belayneh, A., Endale, M., & Eswaramoorthy, R. (2021). Pharmacokinetics and drug-likeness of antidiabetic flavonoids: Molecular docking and DFT study. *PloS one*, *16*(12), e0260853.

[31] Hammam, M.A., Zakaria, Z., Rabee, M., Rabea, A.-T., Hafez, D.E., Abdel-Halim, M., Ismail, A.I. and El-Sayed Mansy, A. (2025), Development of UHPLC-MS/MS Method for Evaluation of the Acute Oral Toxicity and Pharmacokinetics of Ursodeoxycholic Acid and Silymarin Combination in Rats. Sep Sci plus., 8: e202400205.

[32] Ain, Q. U., Saleem, U., Ahmad, B., & Khalid, I. (2023). Pharmacological screening of silibinin for antischizophrenic activity along with its acute toxicity evaluation in experimental animals. *Frontiers in pharmacology*, *14*, 1111915.